UNIVERSITY OF OKLAHOMA

GRADUATE COLLEGE

EVALUATING THE USE OF ENTROPY FIELD DECOMPOSITION IN RESTING STATE FUNCTIONAL MAGNETIC RESONANCE IMAGING ANALYSIS

A THESIS

SUBMITTED TO THE GRADUATE FACULTY

in partial fulfillment of the requirements for the

Degree of

MASTER OF SCIENCE IN ELECTRICAL AND COMPUTER ENGINEERING

By

NISHAAL PARMAR
Norman, Oklahoma
2017

EVALUATING THE USE OF ENTROPY FIELD DECOMPOSITION IN RESTING STATE FUNCTIONAL MAGNETIC RESONANCE IMAGING ANALYSIS

A THESIS APPROVED FOR THE
GALLOGLY COLLEGE OF ENGINEERING

BY

_____
Dr. Hazem Refai, Co-Chair

_____
Dr. Thodur Runolfsson, Co-Chair

_____
Dr. Jerzy Bodurka

Acknowledgements

No research document is a self-contained work. As with any other scientific document, this thesis represents not only my own work, meant to further advance the discoveries of others before me, but also the work of the many others who have advised and aided me in my academic career.

I would like to thank my thesis advisors, Dr. Hazem Refai and Dr. Thodur Runolfsson of the University of Oklahoma, for guiding me through the data analysis techniques used within my thesis, as well as (frequently) providing a welcome contrast to my often pessimistic views on the results of my research. Thank you to Dr. Jerzy Bodurka for instructing me in basic background fMRI knowledge and for serving on my thesis committee. Thank you also to the many OU professors, students, and staff who offered me support and information on a daily basis, and to Michelle Farabough for her assistance.

The data used in this study was acquired by the Laureate Institute for Brain Research (LIBR) in Tulsa Oklahoma in collaboration with scientific director and president Dr. Martin Paulus. LIBR researcher Dr. Rayus Kuplicki provided invaluable assistance in the formation of my initial data analysis scripts, and fellow graduate student Obada Al-Zoubi helped troubleshoot software-related technical difficulties.

Finally, I would like to thank my mother, Anjana, my father, Jitendra, and my brother, Prashant, for their continual care and encouragement in all aspects of my personal and professional life.

Table of Contents

List of Figures

Abstract

The study of resting state functional magnetic resonance imaging (rs-fMRI) data has been the subject of increasing academic interest over the past decade. Despite a growing understanding of the base activity networks (modes) of the human brain, current tools used in rs-fMRI analysis show limited adaptability toward the complexities inherent within intricate and densely connected neural networks. Direct regression analysis is foiled by the multiple, low-SNR, intricate functional networks which characterize the resting state, while advanced analysis methods such as independent component analysis (ICA) are designed to be used on sparse, independent activity signals rather than connected, distributed and overlapping resting state modes.

Entropy Field Decomposition (EFD) is a new analysis technique based on the measurement of neural functional connectivity, rather than neural activity. As an integration of entropy spectrum pathways into information field theory, EFD represents a powerful mathematical method for analyzing the eigenmode connectivity of the brain via local coupling & clustering analysis. EFD may distinguish between non-Gaussian, non-linear, non-periodic, spatially and temporally overlapping signals using the measured space-time correlations present in the data itself.

This thesis explores the method behind the EFD algorithm, then examines a study performed on the effects of the drug ibuprofen on resting state brain function, and uses EFD analysis of subject data to verify the basic viability of the EFD algorithm in fMRI analysis. Although no direct correlation was found between ibuprofen dosage and observed resting state brain response, EFD analysis showed greater functional connectivity in the right hemisphere than in the left hemisphere in nearly all cases.

Chapter 1: An Introduction to Functional Magnetic Resonance Imaging (fMRI) Technology and Techniques

1.1 Purpose of This Thesis

Functional Magnetic Resonance Imaging (fMRI) is a medical imaging technique increasingly used in neurological analysis. A particular focus of recent fMRI literature has been an analysis of commonly observed activity patterns, or 'modes', of the human brain while in a base (resting) state [1]. As these interactions are often complex in both time and space, and they are not tied to an easily observed and repeatable activity, resting state fMRI modes may be difficult to detect and analyze using current techniques. Both direct observation of the blood-oxygenation-level-dependent (BOLD) signal and signal analysis through Independent Component Analysis (ICA) may easily encounter difficulty when analyzing an extended, interconnected, time-dependent neural network. Recently, a new analysis technique known as Entropy Field Decomposition (EFD) has emerged. This method is based on the dynamic connectivity between neural regions. The primary goal of this thesis is to confirm EFD analysis as an available tool for resting state fMRI analysis and to examine its use in fMRI imaging. To accomplish these objectives, EFD analysis will be applied to a medical study comparing resting state fMRI activity between subjects given varying doses of ibuprofen. EFD results will be analyzed for all scans in the study taken as a whole, and also for each individual dosage group. Conclusions of this analysis will be shared, along with suggestions for the possible future use of EFD in fMRI analysis.

1.2 A Brief History of MRI

Magnetic Resonance Imaging (MRI) is a low-risk, noninvasive imaging technique to capture internal anatomical and physiological processes in the presence of a strong magnetic field using the phenomenon of nuclear magnetic resonance (NMR). Unlike other internal medical imaging techniques, MRI does not involve x-rays (used in computed tomography scans), ionizing radiation (used in positron-emission tomography or radiography), or internal instrumentation (used in endoscopies). In the medical field, MRI is frequently used for neurological, cardiovascular, musculoskeletal, and gastrointestinal imaging, as well as in angiography. This diagnostic technique may be used with or without an accompanying contrast agent to shorten T1 relaxation time.

The NMR phenomenon was first discovered in 1946 by Felix Bloch and Edward Purcell [2][3]. In NMR, isotopes containing odd numbers of protons or neutrons will absorb energy in the presence of an external magnetic field, and then re-emit the energy at a specific resonance frequency. The resonance generally occurs in the radio frequency range, the exact frequency depending on the strength of the applied field and excited atom type. This energy may be applied and detected within a strong magnetic field via the use of specialized radiofrequency coils. By combining a strong base magnetic field, along with weaker, perpendicular gradient fields, the spatial location of an excitation may be obtained. This process creates MRI images, which were first discovered by Paul Lauterbur in 1972 and further refined by Peter Mansfield in 1976 [4][5].

1.3 Functional Magnetic Resonance Imaging

Advances in MRI design, coolant systems, and computer hardware enabled the acquisition of increasingly detailed and rapid capture of images, leading to the emergence of fMRI in the late 1990's/early twenty-first century. As such, fMRI research is a relatively new and rapidly expanding area of scientific study. A typical fMRI scanner, such as that used in this thesis' study, contains a field of 3 Tesla (low-field scanners may be 1.5 Tesla, while specialized high-field scanners may be over 9 Tesla), has up to 32-channel reception arrays, and is capable of taking a full-brain image comprised of $8mm^3$ voxels every 2 seconds (typical volume capture times (TRs) in fMRI range from 1 to 3 seconds). [6]

1.4 fMRI Analysis Techniques

At its core, fMRI indirectly measures real-time neural activity through monitoring of the BOLD contrast. As neural activity in a particular region increases, that area of the brain is flooded with additional nutrients in the form of oxygenated hemoglobin via an increased blood flow. The oxygen within the hemoglobin is then consumed to support the increased neural activity [7]. Oxygenated hemoglobin (which is diamagnetic), and deoxygenated hemoglobin (which is paramagnetic), differ in magnetic susceptibility by about 20% and this forms the basis of the BOLD fMRI signal. It is important to note that fMRI is an indirect measure of neural activity; in the case of an active external stimulus, fMRI response via BOLD signal change occurs approximately 3.5 seconds after the stimulus [8].

The most basic, direct form of fMRI analysis involves the study of the BOLD signal, recording which brain regions respond directly after stimulus application and determining which neural regions may be most readily involved with the processing of the stimulus. This direct analysis is most useful when attempting to determine neural processing immediately following a clear, distinct, and repetitive activity, such as repeatedly opening and closing a hand or pressing a button. Statistical analysis, including simple correlation-based [9][10] or more complex regression analysis [11][12], may then be applied using an event-based experiment design with activity-based and non-activity-based periods. The resulting analysis will identify a likely time course of neurological changes directly caused by the chosen stimulus.

Direct fMRI analysis shows only regions with similar signals, thus providing little insight into signal composition. Furthermore, the analysis may often fail to completely capture a complex signal, non-periodic interaction between brain regions, or a signal caused by a more subtle stimulus with components possibly occurring at times other than directly after the initial stimulus. fMRI analysis is further complicated by the following:

- inherent time lag in fMRI measurements between stimulus onset and BOLD response
- connectivity inherent in most neural activity (preventing an ideal setup of independent, orthogonal regressor signals)
- difficulty of 'resetting' neural activity to a desired base level in the often limited time between repeating events

- use of smoothing and loss of unit independence as voxel size grows to either increase the signal-to-noise ratio (SNR) or decrease TR.

Nevertheless, regression analysis remains the most common form of basic fMRI analysis. In regression analysis, several linear regressors, representing various theoretically independent activity pathways including 'noise' regressors to characterize unwanted signal activity (e.g. head movement, respiration, and others) are weighted to form an approximation of the more complex actual fMRI time-signal [13]. A slightly more advanced method of regression analysis, namely Principal Component Analysis (PCA), first attempts to filter out unwanted signals, such as those caused by random noise or respiration. This method again works best with strong, repetitive task-related signals of interest.

The most commonly used advanced fMRI analysis technique is Independent Components Analysis (ICA), which attempts to separate the often low SNR signal of interest and the larger amplitude noise signals. Probabilistic ICA, a modification of the basic ICA algorithm to allow for the investigation of a noisy source signal [14] is currently the most commonly used analysis method for resting state fMRI data [15]. Similar to a basic regression analysis, ICA takes a 4-dimensional fMRI timecourse signal as the input and attempts to break it down into a series of coexisting component signals. Unlike basic analysis methods, multiple spatially overlapping signals may be simultaneously present in any given voxel. In particular, the ICA algorithm splits the base BOLD signal into a specified number of components that are calculated to be maximally independent from one another. Each component represents a single activity pattern allowing for correlation between voxel activity patterns (components) and time-

correlated fluctuation type identification (specific processes including activities and noise). For example, component 1 may be correlated with breathing (noise), component 2 with movement (noise), and component 3 with blinking (activity), possibly the pattern of interest.

Figure 1 shows how each component must be matched to a particular process: the target signal; background noise; type of physiological noise (i.e. movement in each of the 3 axes, respiration); or other factors (e.g. scanner drift, non-target activity processes, task-unrelated noise).

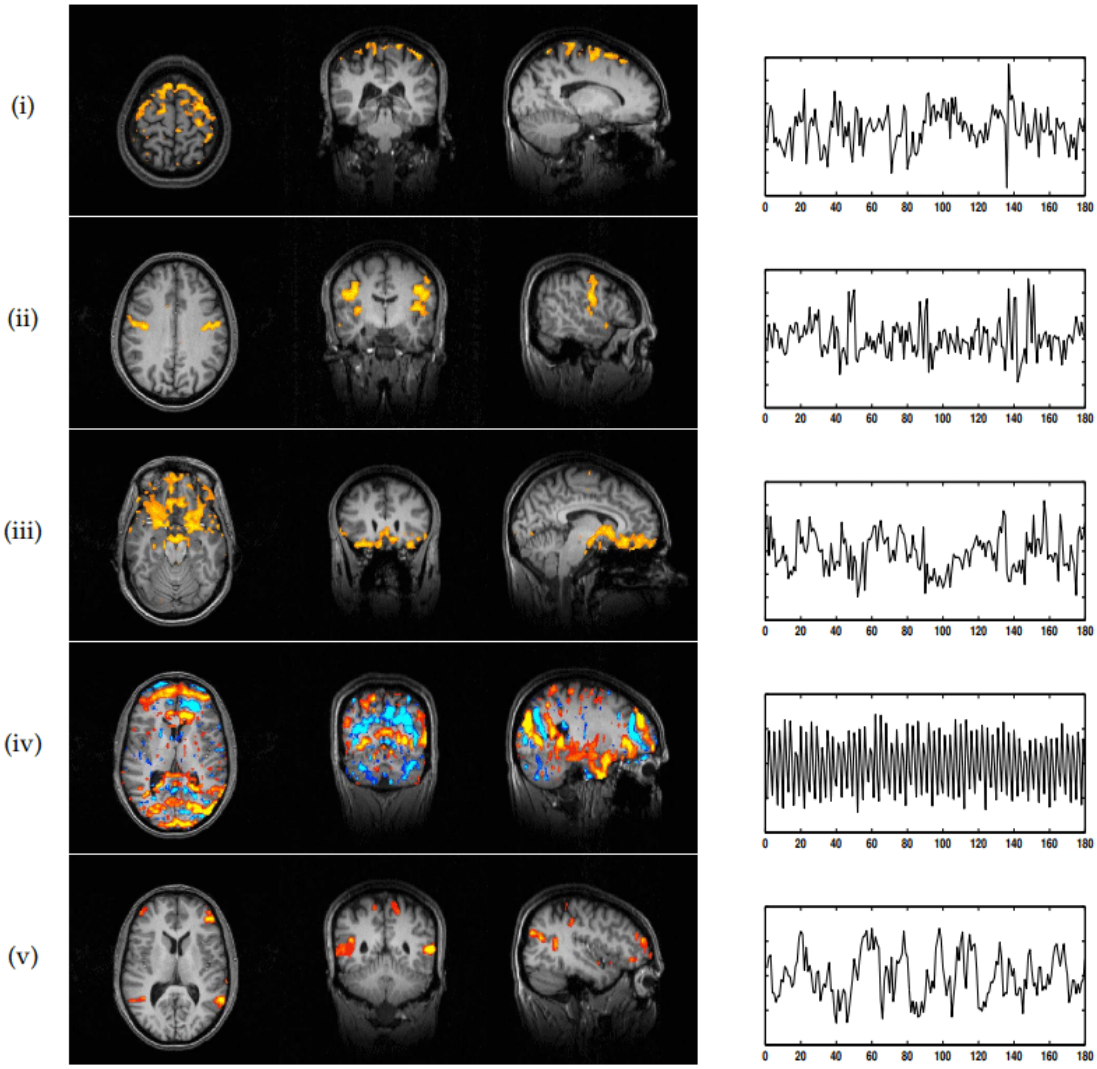

Figure 1: ICA Component Signals From Visual Activation Data
includes (i) head motion (ii) sensory motor activation (iii) signal fluctuations in sinus areas (iv) MR ghost data (v) resting state fluctuations/physiological noise.
Source: Beckman & Smith 2004 [14]

Fundamental functional independence of the task-related signal is once again assumed in ICA analysis [16][17]. The components of a typically noisy fMRI signal include a single signal of interest or a limited number of signals of interest, and many more often higher-amplitude non-task-related noise sources. As the calculated number of components and mathematical dimensionality increase (more clearly differentiating

the signal of interest from additional non-task-related noise sources) ICA signal processing rapidly becomes computationally intensive. To offset this, ICA often uses a "dimensionality reduction" method to decrease computational complexity (PCA, for example) [18]. Furthermore, due to neural activity differences across individuals that result in a unique component pattern for each person analyzed, ICA analysis is much more suited to large-scale studies where data may be aggregated, normalized, and analyzed than it is for a single individual or small-group analysis examining functional differences in individual activity. Any particular ICA component in large-scale studies, although indicative of a population average, may not closely match a given individual's expression of that component. This limits the use of ICA in single-subject analysis. Notably, ICA has been used to characterize resting-state neural connectivity by separating out similar spatial signals with varying timecourses across multiple individuals [19], as well as to establish the currently accepted 7 base resting-state activity modes [20].

1.5 Functional Connectivity and Resting State Analysis

The fundamental difficulty of both direct and ICA analysis lies in the assumption that any given signal of interest and other associated activity data may be separated into a series of identifiable processes that are, ideally, both sparse and independent. Each of these often complex processes must then be able to be correctly correlated to its cause and localized within a given individual [21]. The extremely noisy signal characteristic of fMRI analysis also interferes with the traditional ICA analysis model, further complicating component separation. Unfortunately, no neural

signal exists in isolation, and blind application of the ICA algorithm to fMRI data [22] ignores the signal connectivity of resting state networks. Indeed, the human brain is a vast, intricate network of deeply interconnected neural pathways and regions [23], with significant anatomical and functional differences between individuals. These complex, nonlinear, non-Gaussian, non-independent interactions form the basis of human thought and are, perhaps, most easily observed in the extensive non-task-related neural connectivity networks that define the base non-task-related activity state (resting state) of the human brain. Despite this, many of the most common analysis methods used in resting state neurological studies make basic assumptions which ignore the connected, non-Gaussian nature of resting state activity [24]. Resting state analysis is further complicated by a lack of a single task-related signal that may be effectively isolated, and by the lack of a separate control state for data comparison since the resting state is itself the brain's baseline state. Resting state fMRI studies have become an increasingly examined topic in neurological imaging during the past decade. Unlike in basic activity-based studies, no single brain region or group of regions may be pinpointed as the basis of resting state brain activity.

While an initial analysis and possible identification of these networks may be performed via large-scale group ICA analysis [19][20], an in-depth study of the resting state brain must necessarily involve an increased understanding of the dynamic functional connectivity of the human brain and how each brain region's activation may influence activity patterns in other not necessarily adjacent or physically directly connected brain regions. This functional activity may be exhibited as simple coactivity, in which two functionally connected brain regions often activate and deactivate

together. It may also exhibit as a much more complex system distributed in both spatial and temporal activity.

Despite the vital role of functional connectivity in resting state fMRI studies, until recently, few algorithms have been available to analyze the dynamic connectivity of neural regions in fMRI data. With this in mind, the recently proposed connectivity-based EFD algorithm proposed by Laurence Frank and Vitaly Galinsky in 2016 [25] offers a powerful new analysis technique in the field of resting-state fMRI analysis.

Chapter 2: Entropy Field Decomposition

2.1 Entropy Field Decomposition Background and Advantages

Entropy Field Decomposition (EFD) is a powerful new method of determining the major functional connectivity pathways (modes) of the resting state brain. Unlike direct analysis and ICA, which provide an analysis of brain activity, EFD attempts to analyze the fMRI signal by providing a view of neural connectivity via nearest-neighbor analysis, forming modes of brain regions likely to be functionally connected at any given time. The basic mathematical principles of EFD are derived from information field theory (IFT), a Bayesian method designed to analyze a continuous process using a finite and discrete data sampling of that process. EFD then incorporates prior information into IFT via the integration of entropy spectrum pathways (ESP), resulting in the formation of stable quantized states of signal behavior that are ranked according to their significance. In essence, EFD estimates likely connectivity pathways by taking available data and performing a joint probability analysis between this current data and any prior available connectivity data. Significant eigenvalues of this connectivity matrix represent the steady state connectivity brain modes; less significant eigenvalues represent transition states and system noise.

EFD as an fMRI analysis tool relies upon several base assumptions. The first and most obvious assumption is the existence of commonly expressed functional connectivity pathways within the brain. Furthermore, it is assumed that the brain is commonly found within one of these modes and that transition states between modes are relatively brief. As such, each whole-brain scan may generally be assumed to fall into one or more of these base connectivity modes, with chaotic intermode transition

captures being a relatively rare occurrence. Consequently, once the brain enters a measured connectivity mode, it is much more likely to remain in that mode than it is to transition into a different mode. This lets us determine, via diffusion and connectivity analysis, a number of clearly defined base states with comparatively rare transitions between states. The result provides a stationary probability distribution system for resting state brain connectivity with a series of high probability connectivity modes and a number of relatively low probability transition states.

As a dynamic analysis method based upon functional connectivity, EFD offers many advantages when compared to regression analysis or ICA. Perhaps most relevant to resting state neural analysis, EFD, unlike ICA, readily supports analysis of non-Gaussian, non-linear, non-periodic signals containing multivariate data. Moreover, there is no requirement that these signals be either sparse or independent. EFD is thus superior for detecting spatially and temporally overlapping signals commonly found in resting state fMRI modes, while using only the connectivity and correlation information within the data itself. With EFD, there is no requirement for an external control signal or the input of any prior information.

Figure 2 shows a comparison of ICA and EFD when analyzing a task-based phantom consisting of two spatially overlapping 'activated' regions with additive signals. Note that the EFD algorithm does not inherently assume either signal additivity or Gaussian noise, although both are used in this test. As expected, ICA activity analysis (See Figure 2, bottom row) shows difficulty in distinguishing these overlapping signal regions due to its forcing of maximally independent component signals [26], while EFD connectivity analysis (See Figure 2, middle row), unrestricted by a

preference for sparse and independent signals, accurately separates the two regions by their dynamic connectivity based upon measured correlations within the data.

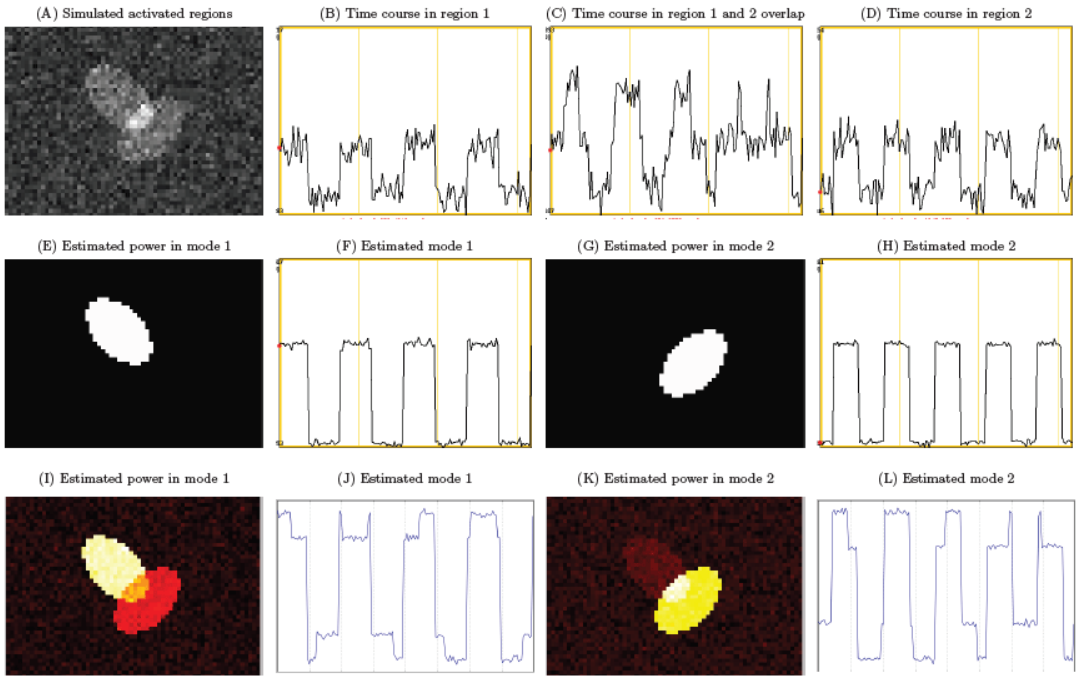

Figure 2: Comparison of EFD With ICA in Task-based fMRI Simulation
(Top) Numerical phantom signal with additive Gaussian noise.
(Mid) Estimated modes using EFD. (Bottom) Estimated modes using ICA.
Source: Frank & Galinsky 2016 [25]

As a connectivity analysis technique, rather than a signal activity decomposition and analysis, EFD offers several additional advantages over ICA. For example, high-dimensionality resting state fMRI data requires significantly less processing time via EFD than ICA, the latter gaining computational complexity extremely rapidly when dealing with high mathematical dimensionality and multiple signal components that span hundreds of thousands of voxels with the short TR of an fMRI system. As a result, EFD analysis may be performed without the ICA voxel smoothing and dimensionality reduction techniques used to reduce computational complexity and noise in ICA.

Likewise, the procedure used to establish connectivity modes via nearest-neighbor analysis will result in an increased SNR in EFD when compared with ICA. EFD modes, with their emphasis on connectivity regions, will often appear to be more uniform, with less noise, lower spatial distribution, and clean well-defined edges compared to their ICA counterparts. Accordingly, EFD requires a slightly higher threshold level for data analysis than ICA (See Figure 3, scan data obtained from [27]). As a result, EFD naturally provides a higher SNR than ICA at identical thresholds [25]. ICA is generally used with larger normalized data sets rather than single-subject analysis, while EFD may be more efficient at demonstrating subject-to-subject modal variation.

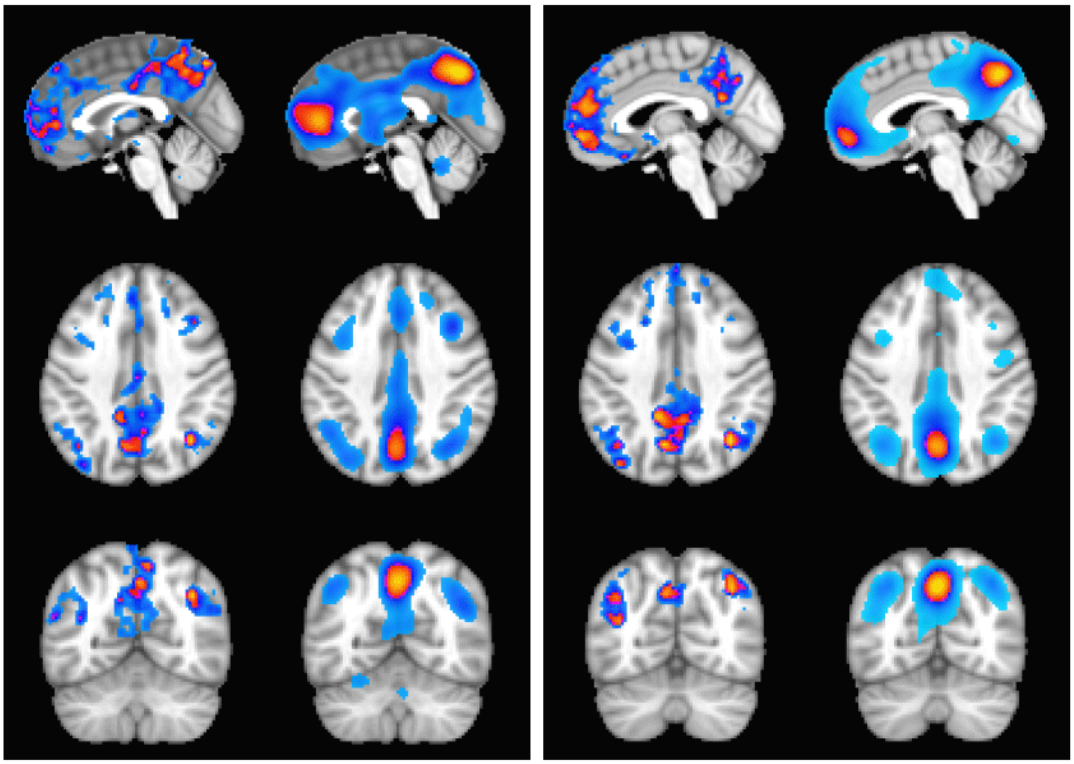

(a) Trial 1, ICA (b) Trial 1, EFD (c) Trial 2, ICA (d) Trial 2, EFD

Figure 3: ICA vs EFD, default mode network, threshold 0.9
Source: Frank & Galinsky 2016 [25]

2.2 Entropy Field Decomposition Mathematical Analysis

The objective of this section is to provide a more numerical analysis of EFD algorithm design. A comprehensive mathematical analysis of EFD, which provides additional details about the derivation of the following equations, may be found in [25][28].

The basic initial input to the EFD algorithm, similar to most fMRI analysis techniques, is the raw discretized BOLD signal capture represented as an array of voxel signal levels with time and space components:

$$d(x_j, t_i) = signal + noise = \hat{R}s(x_j, t_i) + e_{i,j}$$

Also fundamental to EFD is the Bayesian joint probability statistical model used to estimate an unknown signal *s* from a measured dataset *d* and prior information *I*, allowing for future estimation of that unknown signal based on the prior observed evidence:

$$p(s|d, I) = \frac{p(d, s|I)}{p(d|I)} = \frac{p(d|s\ I)\ p(s|I)}{p(d|I)}$$

Re-expressing this joint probability within IFT [29] for a field $\psi(x, t)$ and partition function $p(d|I) = Z(d)$ allows us to apply our discretized data to estimate a continuous signal, giving

$$p(\psi|d, I) = \frac{e^{-H(d,\psi)}}{Z(d)}$$

The information Hamiltonian H above may be written as

$$H(d, \psi) = -\ln p(d, \psi|I) = H_0 - j^{\dagger}\psi + \frac{1}{2}\psi^{\dagger}D^{-1}\psi + H_i(d, \psi)$$

with propagator D, *j* as in information source; H_i representing an interaction Hamiltonian (including terms describing eigenmode interactions, noise, and system response); and H_0 as a normalizing constant [25].

In the case of EFD theory, the prior information consists of information diffusion probabilities calculated via nearest-neighbor coupling. These diffusion probabilities form a ranked probability matrix Q (coupling matrix), of likely connectivity pathways between any two points *i* and *j*. No assumption of Gaussian noise is made within the calculation of the transition probabilities while forming the coupling matrix. This allows for additional flexibility that is inherent in the EFD model. Specifically, transition probability between *i* and *j* along a given eigenvalue path *k* may be expressed as

$$p_{ijk} = \frac{Q_{ji}}{\lambda_k} \frac{\phi_i{}^{(k)}}{\phi_j{}^{(k)}}$$

where λ_k and $\phi^{(k)}$ represent the *k*th eigenvalue and eigenvector of the coupling matrix Q. Using this coupling matrix Q as the prior known data *I* in the IFT signal equation, the estimated IFT signal is calculated:

$$p(s|Q) = \frac{1}{|2\pi Q|^{1/2}} \exp\left(-\frac{1}{2} s_i{}^{\dagger} Q_{ij} s_j\right)$$

Under this model, the definition of a resting state fMRI mode may be expressed as a significant eigenexpansion of the ESP basis fields. An initial cluster of larger eigenvalues represent functional connectivity modes ranked by average duration. The remaining less significant eigenvalues signify system noise and transition states between the significant modes.

To simplify the computing of eigenmodes of the coupling matrix, we may apply a Fourier expansion to the eigenvalue basis functions:

$$\psi(\xi_i) = \sum_{k}^{K} \left[a_k \phi^k(\xi_i) + \ a_k^\dagger \phi^{\dagger,(k)}(\xi_i) \right]$$

We can instead use an ESP expansion in space and a Fourier expansion in time:

$$\psi(x_i, t_j) = \sum_{k,l} a_{k,l} e^{i\omega_l t_j} \phi^{(k,l)} + \ a_{k,l}^\dagger e^{-i\omega_l t_k} \phi^{\dagger,(k,l)}$$

The latter eigenvalue expansion, applied to our coupling matrix Q, becomes:

$$\Lambda a_k = j_k - \sum_{n=1}^{\infty} \frac{1}{n!} \sum_{k_1}^{K} \dots \sum_{k_n}^{K} \widetilde{\Lambda}_{k k_1 \dots k_n}^{(n+1)} a_{k_1} \dots a_{k_n}$$

When factored out in powers of Λ^n, the result is the solution modes as a calculation of eigenvalues and eigenvectors of the coupling matrix. These may be used to determine amplitudes of the interacting coupled connectivity modes as interaction terms of the diagonal eigenvalue matrix:

$$\widetilde{\Lambda}_{k_1 \dots k_n}^{(n)} = \frac{a^{(n)}}{n} \sum_{p=1}^{n} \left(\frac{1}{\lambda_{k_p}} \prod_{m=1}^{n} \lambda_{k_m} \right) \int \left(\prod_{r=1}^{n} \phi^{k_r}(\xi) \right) d\xi$$

Chapter 3: EFD as Applied to a Resting State fMRI Subject Study

3.1 Study Background

The remainder of this thesis discusses the application and analysis of EFD when applied to resting state fMRI data collected in a medical study of the effects of ibuprofen on brain function. Testing was carried out by the Laureate Institute of Brain Research (LIBR), a neurological research institute based in Tulsa, Oklahoma [30]. In this study, performed from July through October 2015, each of 19 healthy adult individuals aged 18 to 55 years old were tested three times, with 1 to 2 weeks between scanning sessions. Three additional subjects did not complete a full series of three scanning sessions, resulting in 61 total fMRI scans with 57 usable sessions. Each subject was given either a placebo (test type A), a 200 mg ibuprofen dose equivalent to a single Advil™ tablet (test type B), or a 600 mg ibuprofen dose (test type C). Each individual received each dose (A, B, and C) once, albeit in a randomized order, and the study itself attempted to determine both overall behavioral response and amygdala activation pattern changes in response to an increasing ibuprofen dose.

Although only the fMRI data was obtained and used in this thesis, each testing session consisted of a multi-part assessment in the following areas:

> "(a) a standardized diagnostic assessment, (b) self-report questionnaires assessing the positive and negative valence domains as well as interoception, (c) behavioral tasks assessing reward-related processing, avoidance, and aversive processing, cognition, and interoception; (d) physiological measurements consisting of facial emotion expression monitoring, heart rate and respiration, (e) functional magnetic resonance imaging focusing on reward-related processing, fear conditioning and extinction, cognitive inhibition, and interoceptive processing, and (f) biomarker assessments." [30]

Each fMRI scan consisted of a scan region of 79x74x94 $8mm^3$ voxels, captured on a 3-Tesla scanner with a TR of 2 seconds. 237 volumes were captured per scan, for

a total scan time of approximately eight minutes per session. Prior to EFD analysis, the subjects' raw fMRI data first underwent standard basic preprocessing, including but not limited to image alignment, motion correction, despiking, and skull stripping. Voxel smoothing or blurring was not used, as this is not needed for EFD analysis. Brain volume for each scan was normalized and co-registered to a shared Talairach anatomical space that consisted of approximately 220,000 voxels of potential interest per capture volume.

3.2 Software Used

Several commonly used software suites were used to process fMRI data. Initial ICA analysis of fMRI data was performed using the FSL MELODIC software suite, commonly utilized in fMRI, MRI, and DTI imaging analysis [31]. Basic viewing of post-EFD fMRI data, as well as clustering analysis, thresholding, and image capture, was accomplished using the AFNI suite, an open-source processing and display environment for functional MRI data developed and maintained by the National Institute of Mental Health [32]. Statistical analysis of the final fMRI data was primarily performed in MATLAB. Finally, the EFD computational tool (and assistance with parameter setup) that was used to analyze the pre-processed fMRI data was provided by Dr. Lawrence Frank at the University of California at San Diego This computational package is the same processing suite used in [25].

3.3 EFD Analysis and Data Processing Methodology

Initial ICA and EFD analysis was first performed on the given preprocessed fMRI study data for all 61 scans. At this point while ICA analysis appeared normal, a key limitation of EFD on the same dataset was observed: as EFD is an analysis of functional connectivity and not signal strength or activity, with over 500,000 voxels in the capture area false positives may easily be mistaken for dominant modes by the EFD algorithm. In particular, on several scans, a region outside the skull consisting of simple background noise was correlated and matched to a primary EFD mode through random chance, with its randomly increasing and decreasing signal matched closely with that of another region's activity pattern. As such, it was necessary to introduce a low-level noise mask to the preprocessed fMRI data before EFD was run. All voxels below a (very low) base noise threshold were set to 0, leaving approximately 220,000 voxels of interest per volume, and effectively removing those regions outside the brain from EFD analysis.

The initial EFD and ICA results were analyzed and used to determine that further research would be concentrated in the examination of the statistical and clustering results of EFD mode 0 across all individuals.

An activity threshold of 94.84% was selected based on clusterization results. This proved to be the minimum threshold level where significant neural activation levels began to separate by brain quadrant (via axial view) or region, rather than remaining in a single large hemispherical or whole-brain cluster (See Figure 4).

At this threshold, a minimum of six significant clusters (over 100 voxels each) were observed in the primary EFD mode of each of the 61 scans. An initial hypothesis

was formed based on initial analysis of the clusterization data and the distribution of clusters along the midaxial brain slice.

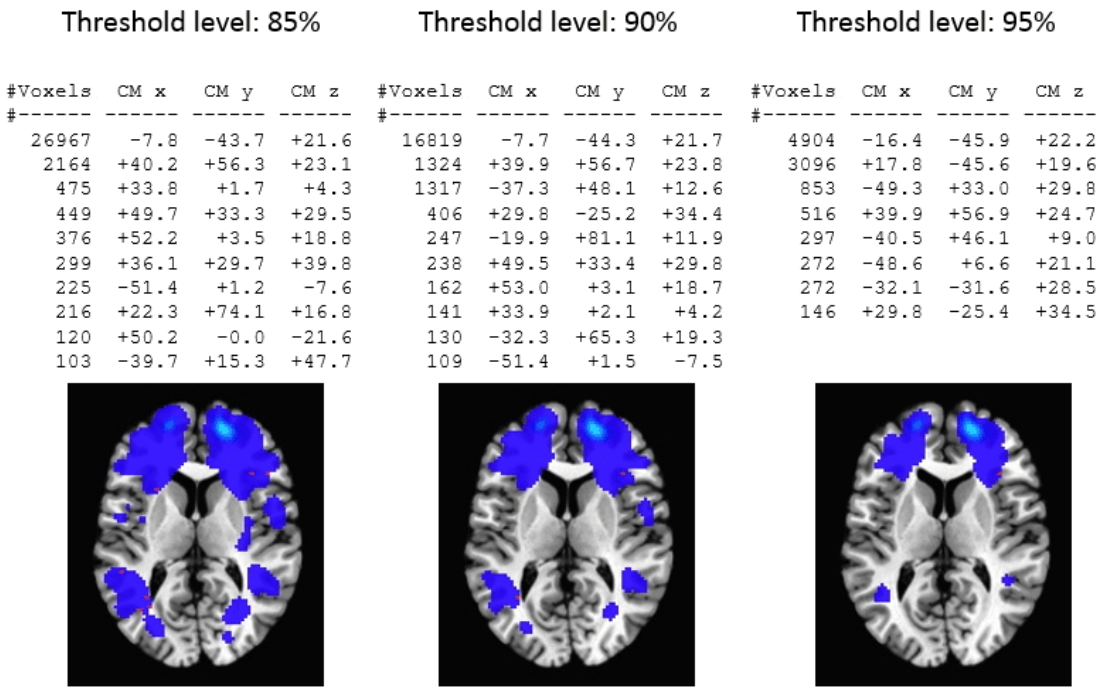

#Voxels	CM x	CM y	CM z
26967	-7.8	-43.7	+21.6
2164	+40.2	+56.3	+23.1
475	+33.8	+1.7	+4.3
449	+49.7	+33.3	+29.5
376	+52.2	+3.5	+18.8
299	+36.1	+29.7	+39.8
225	-51.4	+1.2	-7.6
216	+22.3	+74.1	+16.8
120	+50.2	-0.0	-21.6
103	-39.7	+15.3	+47.7

#Voxels	CM x	CM y	CM z
16819	-7.7	-44.3	+21.7
1324	+39.9	+56.7	+23.8
1317	-37.3	+48.1	+12.6
406	+29.8	-25.2	+34.4
247	-19.9	+81.1	+11.9
238	+49.5	+33.4	+29.8
162	+53.0	+3.1	+18.7
141	+33.9	+2.1	+4.2
130	-32.3	+65.3	+19.3
109	-51.4	+1.5	-7.5

#Voxels	CM x	CM y	CM z
4904	-16.4	-45.9	+22.2
3096	+17.8	-45.6	+19.6
853	-49.3	+33.0	+29.8
516	+39.9	+56.9	+24.7
297	-40.5	+46.1	+9.0
272	-48.6	+6.6	+21.1
272	-32.1	-31.6	+28.5
146	+29.8	-25.4	+34.5

Figure 4: Clustering Threshold Progression (Subject AA104 600mg dose)

Whole-brain activity was analyzed and compared across dosage levels in individual subjects by recording the number of thresholded voxels in each captured axial slice of the primary EFD mode, and then creating a histogram of the connectivity profile for each individual scan. Further statistical whole-brain data was analyzed for each scan, including mean, median, total surviving voxel count, skew, kurtosis, peak information, and relative entropy between dosages. The thresholded volume was then divided by hemisphere and also into four quadrants by slicing along the coronal and sagittal midlines and similar data collected.

Chapter 4: EFD Study Results

4.1 Initial EFD and ICA results

EFD and ICA analysis was run across all 61 scans on a computing cluster provided by LIBR.

ICA analysis yielded normal results, with subject data showing multiple clearly defined modes for each subject scan (See Figure 5). As expected for a single-subject ICA analysis, individual scan ICA modes could not be easily matched to accepted resting state modes, and a great deal of modal variation was observed between subjects (See Figure 6, sample of 4 subject scans), underscoring the unsuitability of ICA for single-subject and small-group resting state fMRI studies.

EFD results were much more consistent, showing clearly similarities in observed modes across multiple subjects (See Figure 7, sample of 4 subject scans). Unlike ICA modes, however, most significant modes observed for individual EFD scans were extremely similar, and may be minor variations of a single dominant resting state connectivity mode (See Figure 8). After reviewing EFD results, due to the low sample size of 19 individuals and the observed similarity between EFD modes, the decision was made focus on the primary EFD mode (mode 0) for further statistical and clustering analysis. Additional investigation into other EFD modes or single-subject ICA results was not pursued.

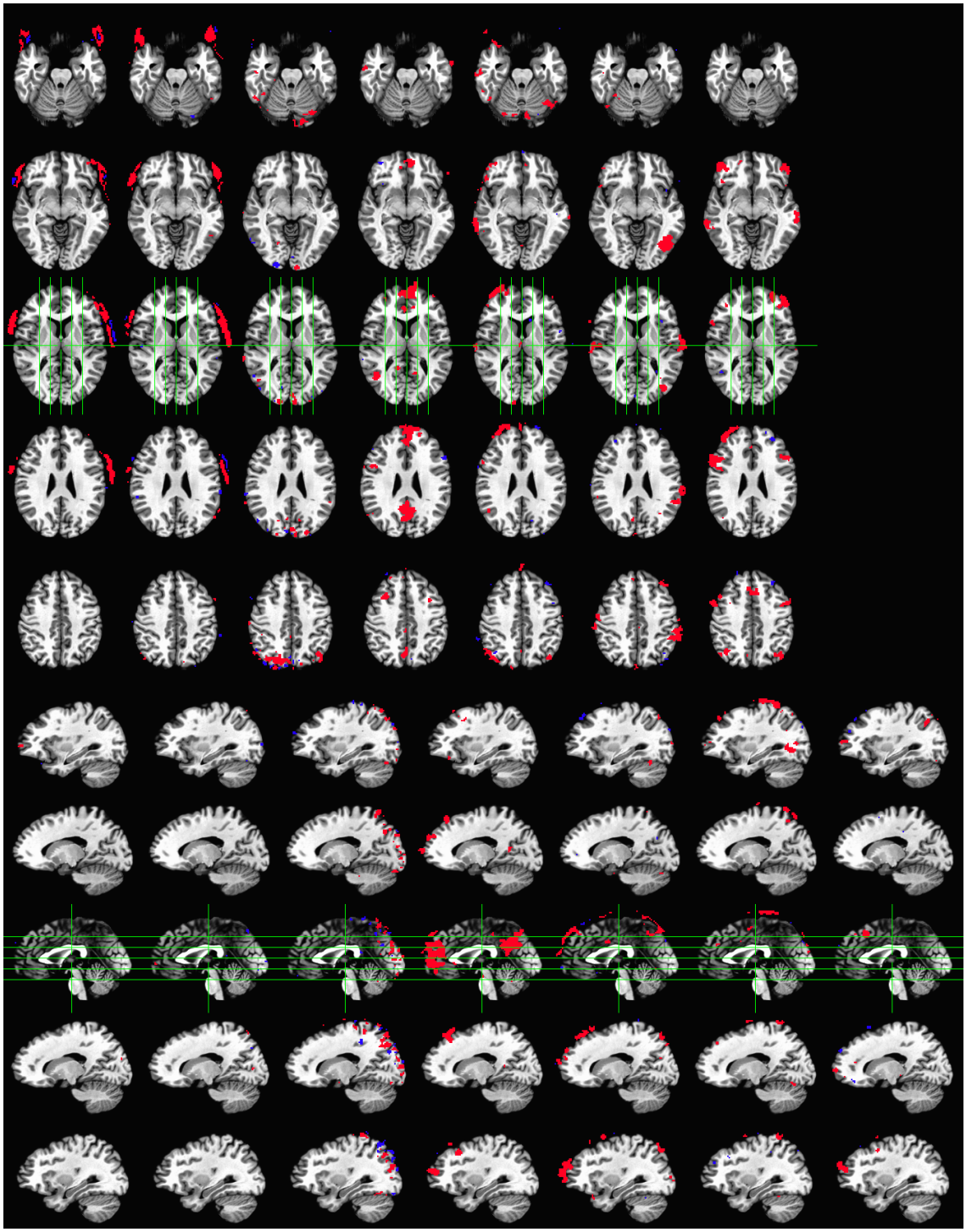

Figure 5: First 7 ICA Modes, Subject AA104, Dosage Group C

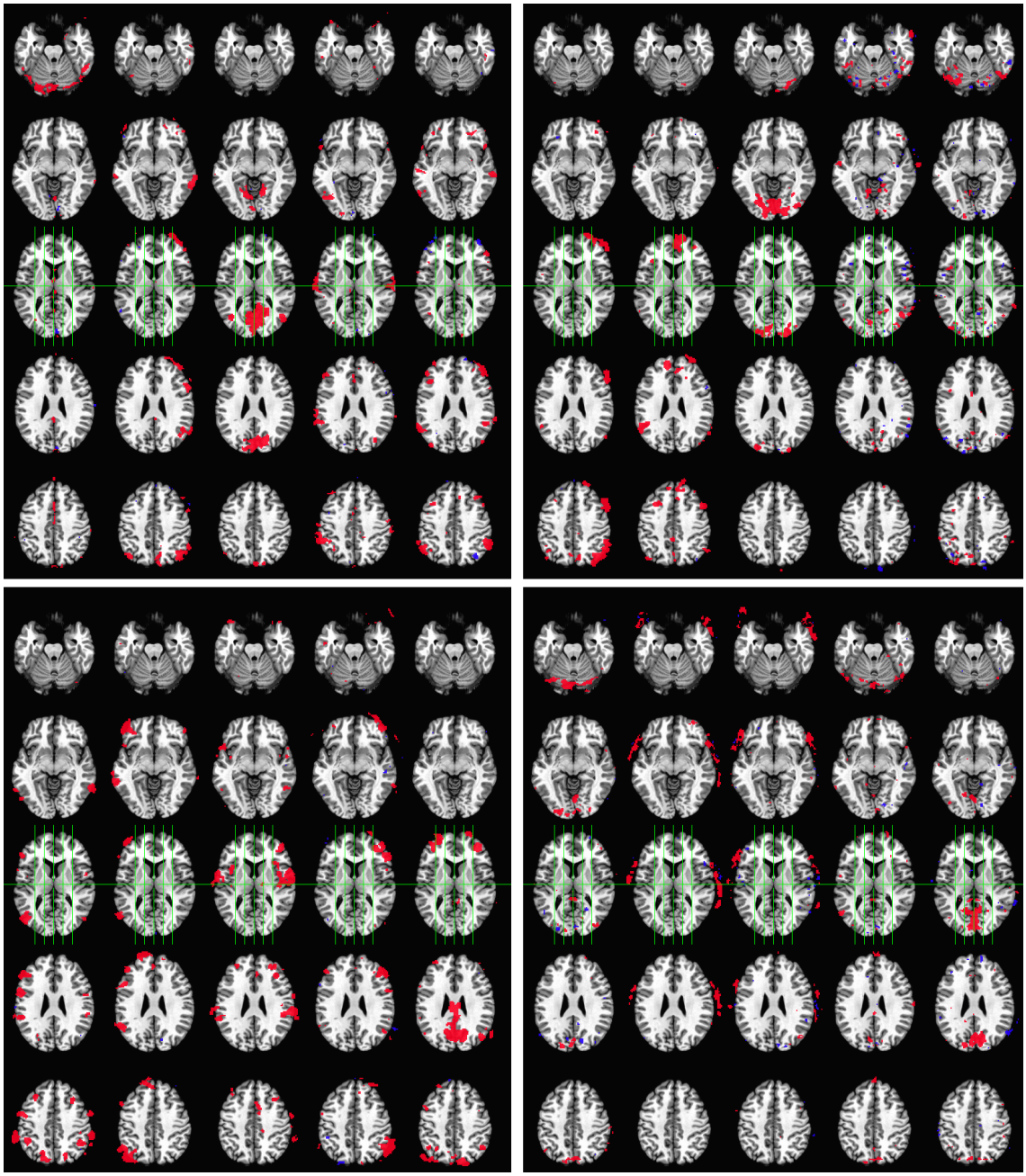

Figure 6: First 5 ICA Modes, 4 Subjects, Dosage Group A
(top left) Subject AA104 (top right) Subject AA115
(bottom left) Subject AA296 (bottom right) Subject AA624

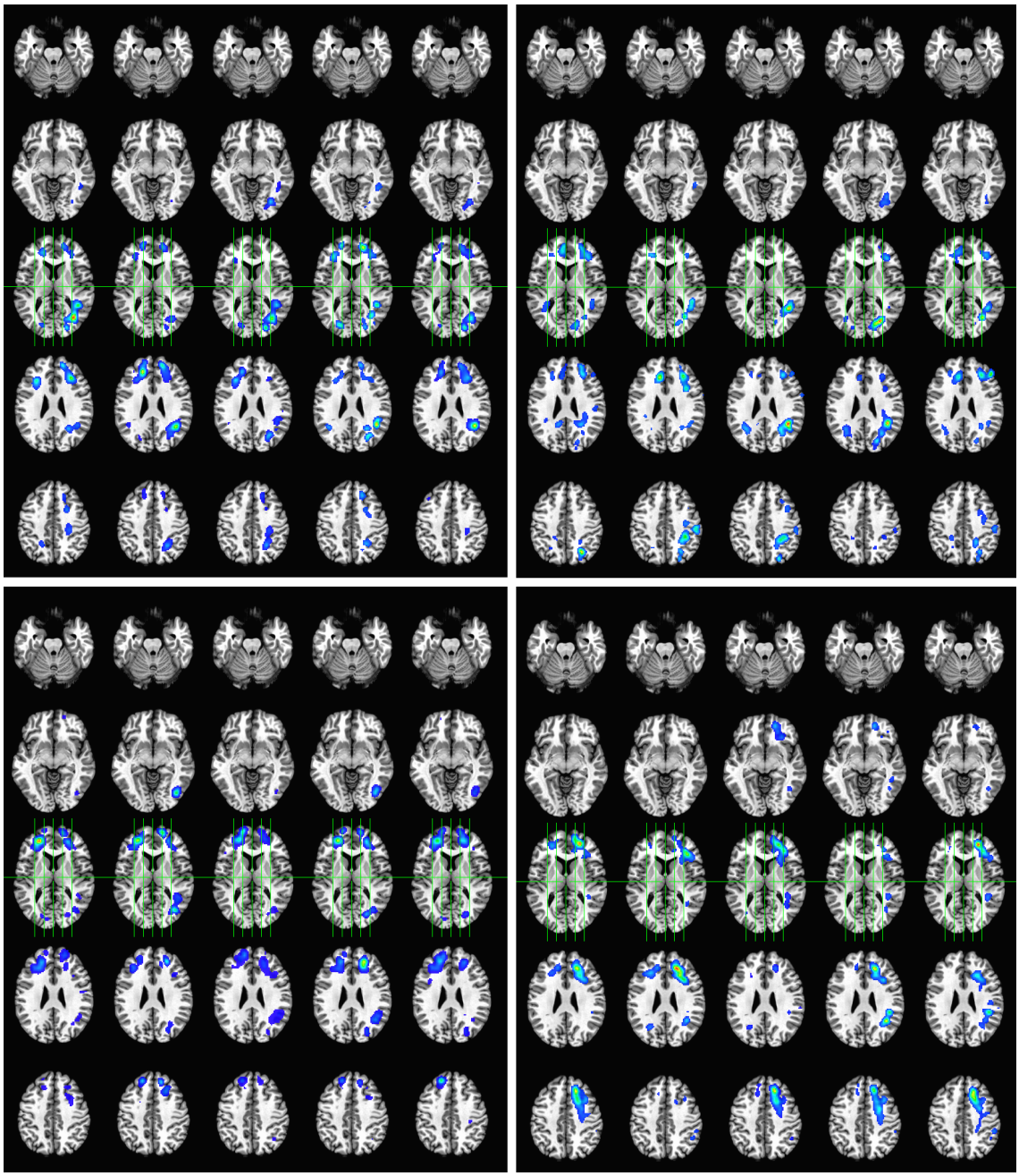

Figure 7: First 5 EFD Modes, 4 Subjects, Dosage Group A
(top left) Subject AA104 (top right) Subject AA115
(bottom left) Subject AA296 (bottom right) Subject AA624

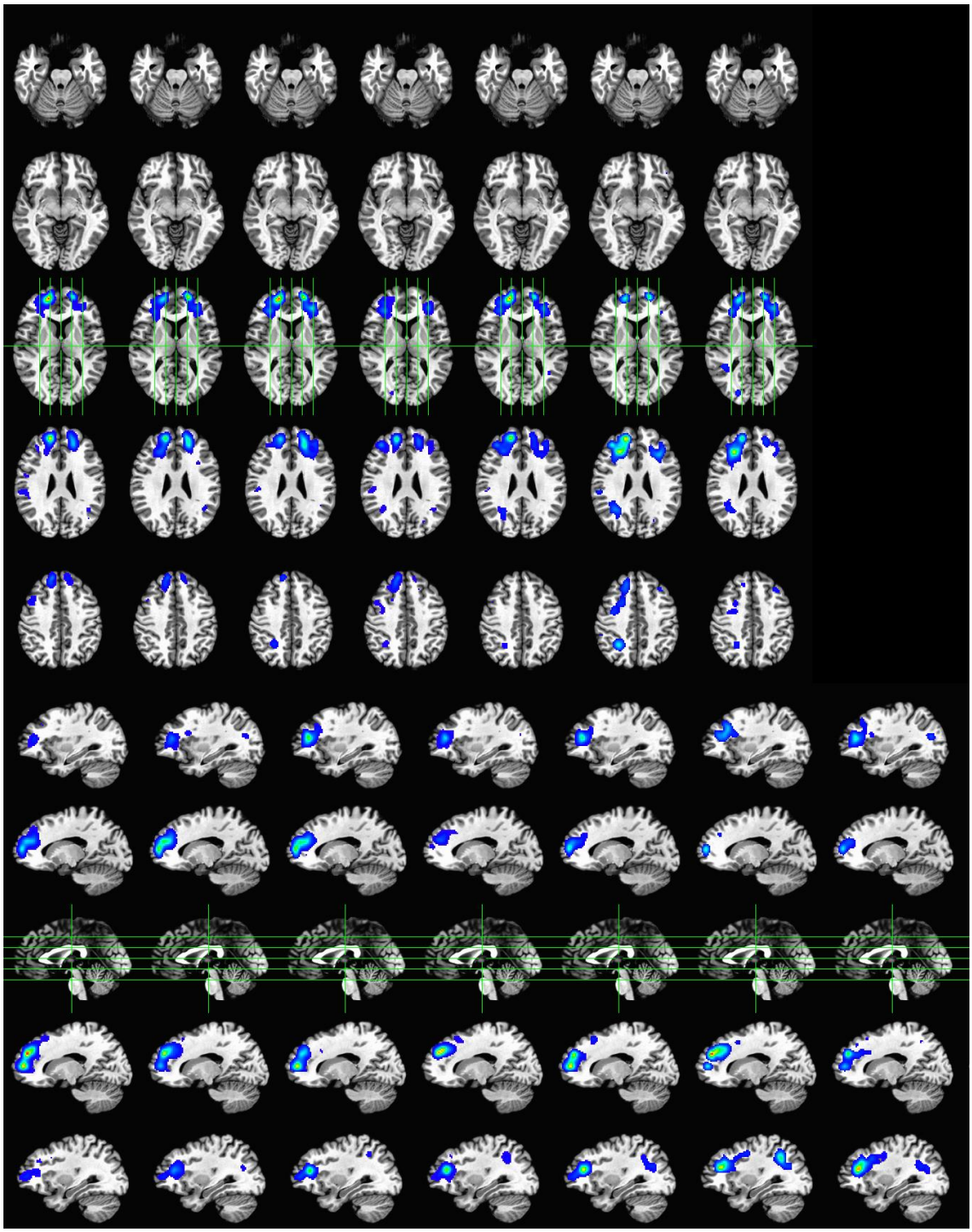

Figure 8: First 7 EFD Modes, Subject AA104, Dosage Group C

4.2 Single Slice and Cluster Analysis

Initial clusterization of EFD mode 0 data at a 94.84% threshold was relatively consistent across all 19 subjects for whom full scan data was collected. A sample clusterization and corresponding midaxial slice is shown in Figure 9 below, and warrants further discussion.

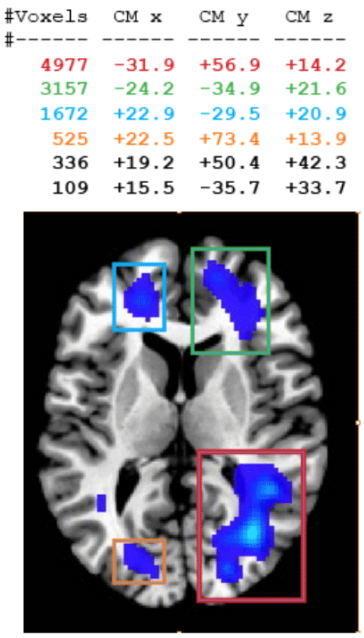

Figure 9: Typical Subject Clusterization Results

Generally, midline axial clusterization across all subject fMRI scans followed a similar pattern, indicative of a shared resting state mode across all subjects. Once a suitably high threshold level was set, four clusters of interest became visible in each subject, one in each axial quadrant. The right hemisphere clusters in particular (outlined in red and green boxes) begin as a single hemisphere-wide cluster, often only separating at high threshold levels, showing a wide range of functional connectivity throughout the hemisphere. The upper clusters (outlined in green and blue boxes) show

the strongest signal and are the last to be lost as threshold levels increase. The bottom left cluster (outlined in an orange box) generally holds the weakest connectivity value, and occasionally disappears from the midline axial view almost entirely by the time the right hemisphere clusters begin separating. As expected for a common mode, the midline axial shape and center-of-mass-location of all four clusters of interest is relatively consistent across all individuals, often with vaguely triangular clusters in the frontal positions (outlined in green and blue). The bottom right cluster (outlined in red) in particular holds a relatively distinctive shape in the midaxial slice across subjects: long and thin, often following the curvature of the brain itself, with three primary connectivity sites often showing strongly in this view.

In 17 of the 19 individuals the midaxial clustering characterization changes in a consistent and predictable manner across the three drug dosage group:
A (placebo, left), B (200mg ibuprofen, middle), and C (600mg ibuprofen, right), as shown in Figure 10.

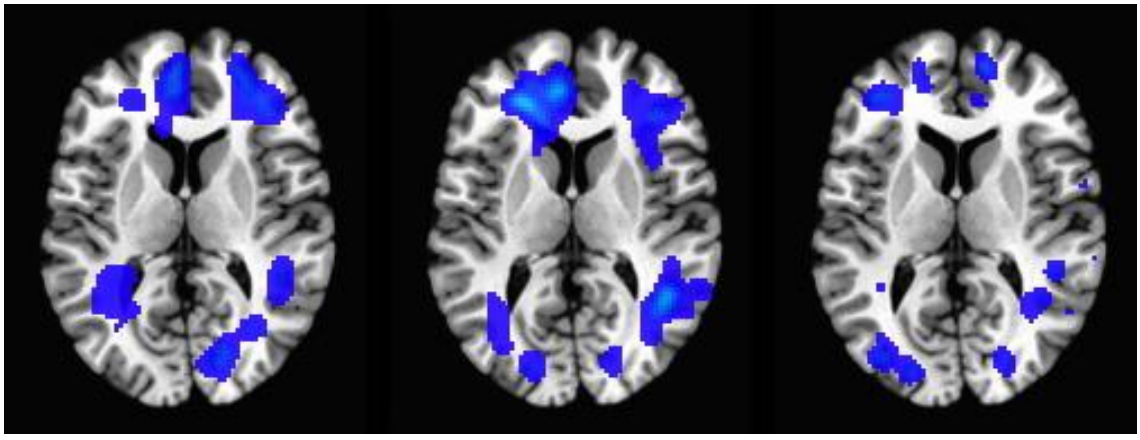

Figure 10: Single-subject Connectivity Variation With Ibuprofen Dosage
(left) Placebo, Group A (mid) 200mg, Group B (right) 600mg, Group C

Generally, as ibuprofen dosage increases, connectivity in the upper right quadrant remains approximately the same or decreases, as does the connectivity of the lower right quadrant. Additionally, the activity in the lower right quadrant becomes more sporadic in nature and often moves further toward the mid-hemisphere region, occasionally moving into or slightly above the midline.

These results aided in the formation of an initial hypothesis regarding the effects of ibuprofen on resting state functional connectivity: as subjects receive a substantial drug dose, we expect to see a change in brain activity from a given mode configuration (base-type) to a slightly but noticeably different configuration (modified-type). Depending on the differing nature of painkiller drug resistance between subjects, we hypothesize that the actual functional connectivity of our subjects to start with the base-type when given a placebo, then change toward the modified-type to some degree based on drug resistance at the 600mg dose. Results from the 200mg dose should fall somewhere in between. Under this hypothesis, subject results such as those in Figure 10 would exhibit low drug resistance, while subjects with relatively consistent connectivity across all three dosages would exhibit higher drug resistance.

4.3 Whole Brain Statistical Analysis

Moving away from clusterization analysis and a more subjective study of the midline axial slice, the connectivity profile of the primary EFD mode (again thresholded to 94.84%) across the entire brain volume may be visually characterized (See Figure 11) by creating a histogram-like graph of individual fMRI scans. The number of post-threshold surviving voxels was graphed against the axial slice position

in which they are located. Figure 11 shows the primary-mode EFD profiles (identified by a solid line) across four individuals (AH072, AH307, AH490, AH645) for all dosages. The top row depicts dosage group A (placebo); the middle shows group B (200mg ibuprofen); the bottom demonstrates group C (600mg ibuprofen). For reference, the dotted line represents the number of potential voxels of interest across the entire brain region, also normalized to the 94.84% threshold of the EFD analysis.

If the hypothesis from the previous section holds, each subject (detailed in columns) should show either consistent connectivity profiles across all three dosages (detailed in rows) for subjects who exhibit high drug resistance. Alternatively, profiles should all change gradually and predictably moving from the placebo dose to the 600mg dose for subjects with low drug resistance. Unfortunately, no clear pattern emerges within the connectivity profiles, and no clear trend may be discerned at the subject level between various dosages.

A numerical analysis of these histograms again fails to identify any clear functional connectivity progression linked to drug dosage (See Figure 12). Of particular note in this numerical analysis is the calculation of the relative entropy of 200 and 600mg drug dosage graphs when compared with the placebo dose for each individual. Relative entropy, also known as the Kullback-Leibler divergence, is a measure of how greatly (measured along a logarithmic scale) a probability distribution differs from a second expected probability distribution function (pdf). By normalizing the graphed histograms to a unit area, a probability distribution may be obtained for each fMRI connectivity analysis.

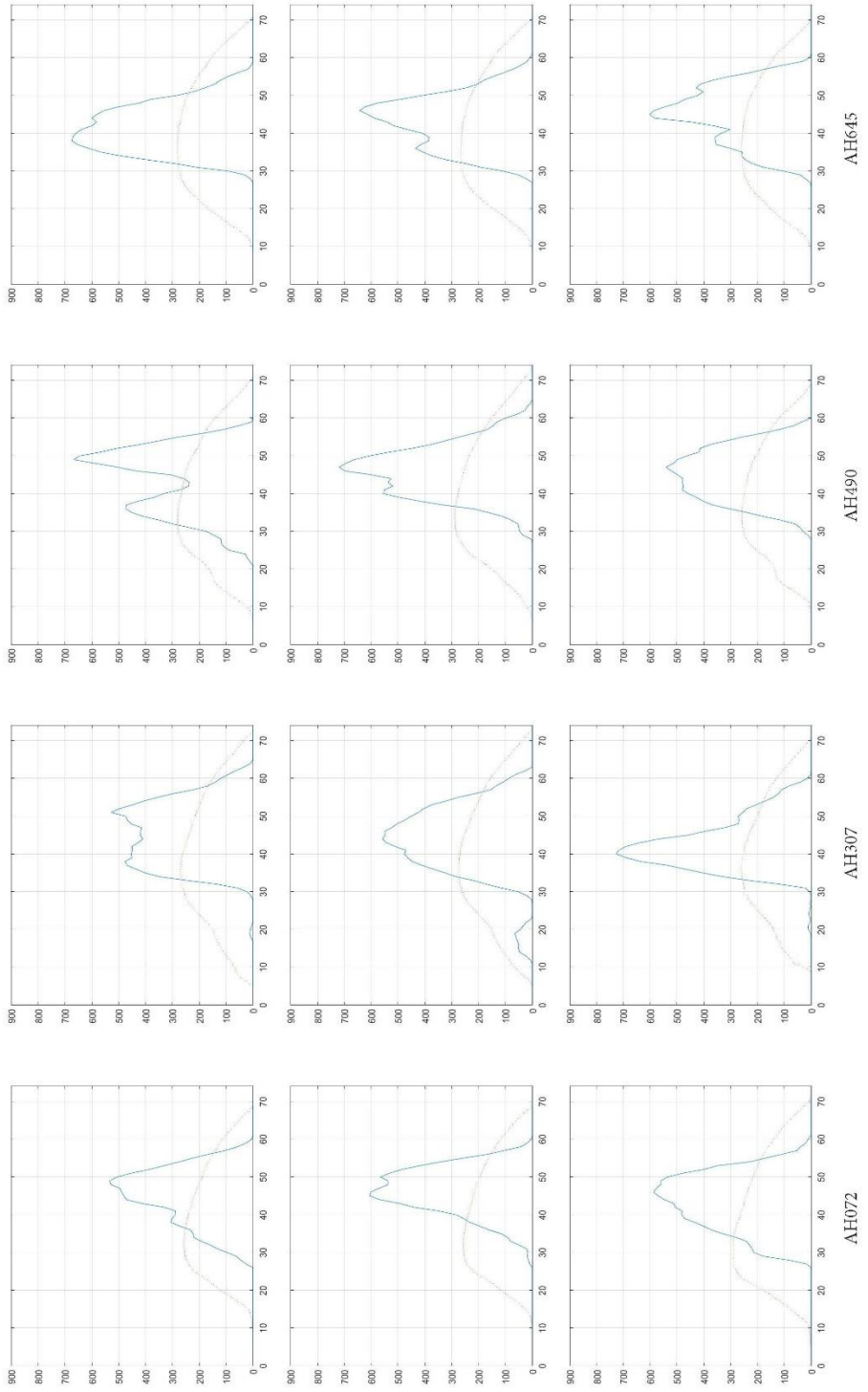

Figure 11: Histogram Graphs of Primary Mode EFD Connectivity; Surviving Connected Voxels vs. Axial Position

Figure 12: Numerical Analysis of Histogram Data in Figure 8

In line with the initial hypothesis, and setting the placebo ibuprofen dosage graph as our baseline distribution, we would expect individuals with a high drug resistance to have little variation in relative entropy between dosages, while individuals with low drug resistance would see a consistent change in relative entropy at a high dosage. The 200mg dosage relative entropy value should fall in between. Instead, relative entropy results preclude the formation of a strong correlation between resting state primary mode functional connectivity profiles and ibuprofen dosage by exhibiting remarkably evenly scattered relative entropy results across the three possibly broad categories; of the 19 individuals analyzed, 5 show relative equal relative entropy across all dosage levels; 7 show increasing entropy from placebo to high dosage, with the low dosage level in between; and frustratingly, 7 show significantly greater relative entropy with low-dosage ibuprofen than high-dosage when compared to the placebo pdf.

Repeating both the visual and numerical analysis for each quadrant individually yields similar results, again showing no discernable trend propagating through drug dosage levels on the individual level. Nearly even relative entropy results are demonstrated across all reasonable statistical analysis categories, once again preventing the drawing of any consistent conclusions between ibuprofen dose and EFD functional connectivity modes.

4.4 Total Activity by Hemisphere

A final observation may be made when calculating the total thresholded connectivity levels per hemisphere for each subject (See Figure 13). In 53 of 57 counts of surviving voxels post-thresholding in the primary EFD mode, the right hemisphere shows more functional connectivity than the left hemisphere. For the four cases in which this phenomenon did not hold, subsequent scans of the same subject with a different ibuprofen dosage again followed this trend toward right-hemisphere-connectivity dominance.

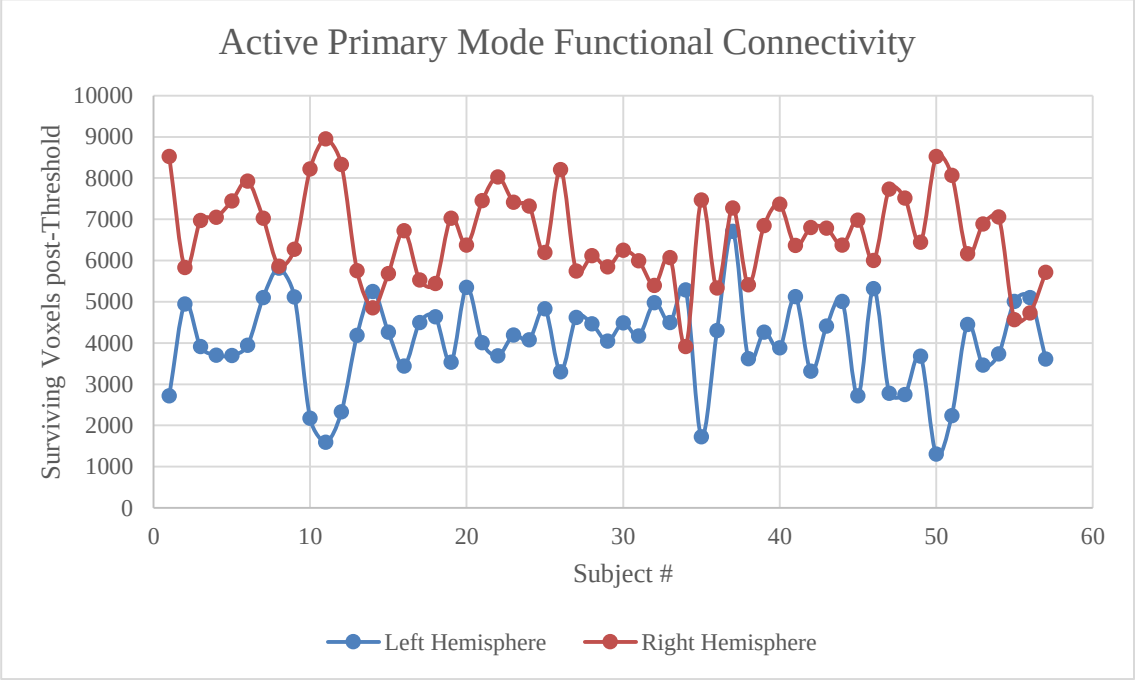

Figure 13: Functional Connectivity: Surviving Voxels by Hemisphere

This observation provides independent support for a previous Near-Infrared Spectroscopy (NIRS) [33] study which concluded that resting state brain activity is inherently asymmetrical, regardless of right vs. left-handedness or other physical

characteristics, with most subjects showing greater resting state connectivity in the right hemisphere.

Chapter 5: Conclusions and Future Work

5.1 Conclusions

Most importantly, this thesis establishes the base viability of the EFD algorithm for resting state fMRI studies. EFD provides reliable, consistent, and reproducible results in the examination of resting state neural connectivity modes. As a connectivity-based algorithm, rather than an activity based analysis, EFD offers particular strengths in analyzing the complex, non-Gaussian, dense, and highly interconnected dynamic networks which characterize resting state brain activity. While a direct link between ibuprofen dosage and functional connectivity changes was unable to be established using EFD analysis, we were able to provide confirmation via an independent analysis (EFD) of the dominance of right-hemisphere functional connectivity in the primary resting state neural mode.

5.2 Future Work

Two further avenues of study into the use of EFD for neuroimaging analysis are suggested as a natural extension of this thesis.

The first opportunity involves the classification and characterization of multiple resting state fMRI modes via EFD. While this thesis focused on the primary EFD mode network, a large-scale study similar to the 1000-scan ICA analysis in [20] has not been conducted via EFD analysis to confirm the existence of the seven commonly-accepted resting state neural modes.

The second opportunity involves the direct comparison of ICA and EFD. This would most easily be accomplished by comparing the performance of both algorithms

in the analysis of simple task-related data. Experiment task blocks would consist of simple activities such as blinking, button pressing, and hand opening/closing, with easily isolated BOLD signal activity perturbations which may be assumed to be closely related to the target activity's functional connectivity.

While much work remains to be done before EFD becomes a widely accepted tool for fMRI analysis, this study nonetheless represents a powerful new advanced analysis technique for the discovery of functional neurological connectivity networks.

References

[1] Buckner, Randy L., and Justin L. Vincent. "Unrest at rest: default activity and spontaneous network correlations." *Neuroimage* 37.4 (2007): 1091-1096.

[2] Bloch, Felix. "Nuclear induction." *Physical review* 70.7-8 (1946): 460.

[3] Purcell, Edward M., H. Co Torrey, and Robert V. Pound. "Resonance absorption by nuclear magnetic moments in a solid." *Physical review* 69.1-2 (1946): 37.

[4] Lauterbur, P. C. "Image Formation by Induced Local Interactions: Examples Employing Nuclear Magnetic Resonance." *Nature* 242.190 (1973): 191.

[5] Mansfield, P., and A. A. Maudsley. "Line scan proton spin imaging in biological structures by NMR." *Physics in medicine and biology*21.5 (1976): 847.

[6] "Imaging and Information Technology" http://www.laureateinstitute.org/technology.html Accessed October 2017.

[7] Ogawa, Seiji, et al. "Oxygenation-sensitive contrast in magnetic resonance image of rodent brain at high magnetic fields." *Magnetic resonance in medicine* 14.1 (1990): 68-78.

[8] Blamire, Andrew M., et al. "Dynamic mapping of the human visual cortex by high-speed magnetic resonance imaging." *Proceedings of the National Academy of Sciences* 89.22 (1992): 11069-11073.

[9] Biswal, Bharat, et al. "Functional connectivity in the motor cortex of resting human brain using echo-planar mri." *Magnetic resonance in medicine* 34.4 (1995): 537-541.

[10] Fransson, Peter, and Guillaume Marrelec. "The precuneus/posterior cingulate cortex plays a pivotal role in the default mode network: Evidence from a partial correlation network analysis." *Neuroimage* 42.3 (2008): 1178-1184.

[11] Logothetis, Nikos K., et al. "Neurophysiological investigation of the basis of the fMRI signal." *Nature* 412.6843 (2001): 150-157.

[12] Greicius, Michael D., et al. "Functional connectivity in the resting brain: a network analysis of the default mode hypothesis." *Proceedings of the National Academy of Sciences* 100.1 (2003): 253-258.

[13] Friston, Karl J., et al. "Statistical parametric maps in functional imaging: a general linear approach." *Human brain mapping*2.4 (1994): 189-210.

[14] Beckmann, Christian F., and Stephen M. Smith. "Probabilistic independent component analysis for functional magnetic resonance imaging." *IEEE transactions on medical imaging*23.2 (2004): 137-152.

[15] Smith, Stephen M., et al. "Resting-state fMRI in the human connectome project." *Neuroimage* 80 (2013): 144-168.

[16] Bell, Anthony J., and Terrence J. Sejnowski. "An information-maximization approach to blind separation and blind deconvolution." *Neural computation* 7.6 (1995): 1129-1159.

[17] Comon, Pierre. "Independent component analysis, a new concept?" *Signal processing* 36.3 (1994): 287-314.

[18] Calhoun, V. D., et al. "Spatial and temporal independent component analysis of functional MRI data containing a pair of task-related waveforms." *Human brain mapping* 13.1 (2001): 43-53.

[19] Beckmann, Christian F., et al. "Investigations into resting-state connectivity using independent component analysis." *Philosophical Transactions of the Royal Society of London B: Biological Sciences* 360.1457 (2005): 1001-1013.

[20] Yeo, BT Thomas, et al. "The organization of the human cerebral cortex estimated by intrinsic functional connectivity." *Journal of neurophysiology* 106.3 (2011): 1125-1165.

[21] Smith, Stephen M., et al. "Resting-state fMRI in the human connectome project." *Neuroimage* 80 (2013): 144-168.

[22] McKeown, Martin J., et al. *Analysis of fMRI data by blind separation into independent spatial components*. No. NHRC-REPT-97-42. NAVAL HEALTH RESEARCH CENTER SAN DIEGO CA, 1997.

[23] Tononi, Giulio, Olaf Sporns, and Gerald M. Edelman. "A measure for brain complexity: relating functional segregation and integration in the nervous system." *Proceedings of the National Academy of Sciences* 91.11 (1994): 5033-5037.

[24] Kolchinsky, Artemy, et al. "Multi-scale integration and predictability in resting state brain activity." *Frontiers in neuroinformatics* 8 (2014).

[25] Frank, Lawrence R., and Vitaly L. Galinsky. "Dynamic multiscale modes of resting state brain activity detected by entropy field decomposition." *Neural computation* (2016).

[26] Calhoun, Vince D., et al. "Independent component analysis for brain fMRI does indeed select for maximal independence." *PloS one* 8.8 (2013): e73309.

[27] Shehzad, Zarrar, et al. "The resting brain: unconstrained yet reliable." *Cerebral cortex* 19.10 (2009): 2209-2229.

[28] Frank, Lawrence R., and Vitaly L. Galinsky. "Information pathways in a disordered lattice." *Physical Review E* 89.3 (2014): 032142.

[29] Enßlin, Torsten A., Mona Frommert, and Francisco S. Kitaura. "Information field theory for cosmological perturbation reconstruction and nonlinear signal analysis." *Physical Review D* 80.10 (2009): 105005.

[30] "Study of Ibuprofen Effects on Brain Function" [Online]. Available: https://clinicaltrials.gov/ct2/show/NCT02507219

[31] "FSL – FMRIB Software Library" [Online]. Available: https://fsl.fmrib.ox.ac.uk/fsl/fslwiki/

[32] "AFNI – Analysis of Functional NeuroImages" [Online]. Available: https://afni.nimh.nih.gov/

[33] Medvedev, Andrei V. "Does the resting state connectivity have hemispheric asymmetry? A near-infrared spectroscopy study." *Neuroimage* 85 (2014): 400-407.